

# In Situ NMR Observations of the Photolysis of Cymantrene and Methylcymantrene in Supercritical Fluids: A New Technique Using High-Pressure NMR

John C. Linehan,<sup>\*,†</sup> Scott L. Wallen,<sup>†,‡</sup> Clement R. Yonker,<sup>†</sup>  
Thomas E. Bitterwolf,<sup>‡</sup> and J. Timothy Bays<sup>‡</sup>

Contribution from the Chemical Sciences Department, Pacific Northwest National Laboratory,<sup>§</sup> Richland, Washington 99352, and the Department of Chemistry, University of Idaho, Moscow, Idaho 83844-2343

Received April 14, 1997<sup>⊗</sup>

**Abstract:** The *in situ* photolytic exchange of ethylene and hydrogen for carbon monoxide on cymantrene (CpMn(CO)<sub>3</sub>, Cp =  $\eta^5$ -cyclopentadienyl) and methylcymantrene (MeCpMn(CO)<sub>3</sub>, MeCp = monomethyl- $\eta^5$ -cyclopentadienyl) dissolved in subcritical and supercritical solvents (CO<sub>2</sub> and ethylene) was investigated by high-resolution, high-pressure <sup>1</sup>H NMR over the temperature range from -40 to 150 °C and a pressure range from 35 to 2600 bar. Photolytic substitution of ethylene for CO proceeded to completion under all conditions investigated, and only one ethylene was observed to substitute for CO on the manganese complexes even in neat ethylene under extreme conditions of pressure and temperature. Only small amounts of dihydrogen were observed to substitute for CO on cymantrene at 35 °C in a binary solvent mixture of CO<sub>2</sub>/H<sub>2</sub> during photolysis. The <sup>1</sup>H chemical shifts of the manganese complexes and their ethylene substituted products were found to be linearly dependent on density with temperature and solvent dependence also observed. The spin-lattice relaxation times (*T*<sub>1</sub>) of all the solvent and solute species were observed to be inversely proportional to the density of the solvent over the range of conditions investigated. Temperature and concentration dependent phase behavior and solute saturation were also determined for the methylcymantrene and MeCpMn(CO)<sub>2</sub>( $\eta^2$ -C<sub>2</sub>H<sub>4</sub>) solutes in SCF ethylene. These results represent the first NMR detected *in situ* photolysis study of organometallics in SCF and demonstrate the utility of this technique.

## Introduction

Interest in supercritical fluids (SCF) has grown enormously in the past decade, which is understandable from both fundamental and technological points of view since the densities and transport properties of a fluid can be *continuously* varied between gas-like and liquid-like values. This allows the study of intermolecular interactions over a wide range of molecular distances and the tuning of the solvation properties of the fluid. More recently a number of studies have focused on the use of supercritical fluids as reaction media and reactants for organometallic reactions:<sup>1–3</sup> in particular, the utility of SCF in the production of normally unstable or hard to synthesize organometallic species,<sup>4</sup> the elucidation of mechanistic pathways in hydroformylation,<sup>5</sup> and as solvents for asymmetric catalysis.<sup>6,7</sup> Several of these studies have been directed toward understanding the fundamental properties and reactions of photochemical substitution of ligands on organometallic complexes in SCF. The majority of the experimental evidence concerning the fate

of reactants comes from *ex situ* analysis of the reaction products<sup>1</sup> or indirect *in situ* observations of the binding of substituted ligands to the metal center by monitoring the carbon monoxide stretching vibrations with FTIR spectroscopy.<sup>2,4</sup> However, the direct observation of the substituted ligands on the metal center through *in situ* NMR has not heretofore been reported.

We have developed an inexpensive pressure vessel compatible with the *in situ* spectroscopic observation of species in SCF by NMR,<sup>8,9</sup> ESR,<sup>8</sup> and XAFS<sup>10</sup> that can withstand pressures up to 4000 bar. Commercially available fused silica capillary tubing is well suited for the investigations of fluids under extreme conditions due to the capillary's high tensile strength caused by the high o.d.-to-i.d aspect ratio. A discussion on the strength of glass as a function of the wall thickness-to-inside diameter ratio has previously been given by Yamada.<sup>11</sup> The high-pressure NMR (HPNMR) capillary cell was recently demonstrated to be an excellent vessel for the NMR detected observations of *in situ* photolysis reactions due to favorable optical, as well as magnetic, properties.<sup>12</sup> In the present study, we investigate the stability and reactivity of cymantrene and methylcymantrene in SCF under extreme conditions and offer the first demonstration of photolysis in high-pressure SCF with *in situ* NMR detection of the substitution reactions on organometallic complexes by ethylene and hydrogen. We also illustrate the use of

(8) Spectrometer Capillary Vessel and Method of Making Same, U.S. Patent No. 5,469,061, 1995.

(9) Yonker, C. R.; Wallen, S. L.; Linehan, J. C. *J. Supercrit. Fluids* **1995**, *8*, 250–254.

(10) Wallen, S. L.; Pfund, D. M.; Fulton, J. L.; Yonker, C. R.; Newville, M.; Ma, Y. *Rev. Sci. Instrum.* **1996**, *67*, 2843–2845.

(11) Yamada In *Glass Cell Method for High-Pressure High Resolution NMR Measurements. Applications to the Studies of Pressure Effects on Molecular, Conformation and Structure*; Diehl, P., Fluck, E., Gunther, H., Kosfeld, R., Seelig, J., Springer-Verlag: Berlin, 1991; pp 233–263.

(12) Yonker, C. R.; Wallen, S. L. *Appl. Spectrosc.* **1996**, *50*, 781–784.

<sup>†</sup> Pacific Northwest National Laboratory.

<sup>‡</sup> University of Idaho.

<sup>§</sup> Operated by Battelle Memorial Institute.

<sup>⊗</sup> Current address: Department of Chemistry, CB# 3290, University of North Carolina, Chapel Hill, NC 27599.

<sup>⊗</sup> Abstract published in *Advance ACS Abstracts*, August 15, 1997.

(1) Jessop, P. G.; Ikariya, T.; Noyori, R. *Science* **1995**, *269*, 1065–1069.

(2) Poliakoff, M.; Howdle, S. M.; Kazarian, S. G. *Angew. Chem., Int. Ed. Engl.* **1995**, *34*, 1275–1295.

(3) Jessop, P. G.; Ikariya, T.; Noyori, R. *Organometallics* **1995**, *14*, 1510–1513.

(4) Banister, J. A.; Lee, P. D.; Poliakoff, M. *Organometallics* **1995**, *14*, 3876–3885.

(5) Klinger, R. J.; Rathke, J. W. *J. Am. Chem. Soc.* **1994**, *116*, 4772.

(6) Burk, M. J.; Feng, S.; Gross, M. F.; Tumas, W. *J. Am. Chem. Soc.* **1995**, *117*, 8277–8278.

(7) Jessop, P. G.; Hsiao, Y.; Ikariya, T.; Noyori, R. *J. Am. Chem. Soc.* **1996**, *118*, 344–355.

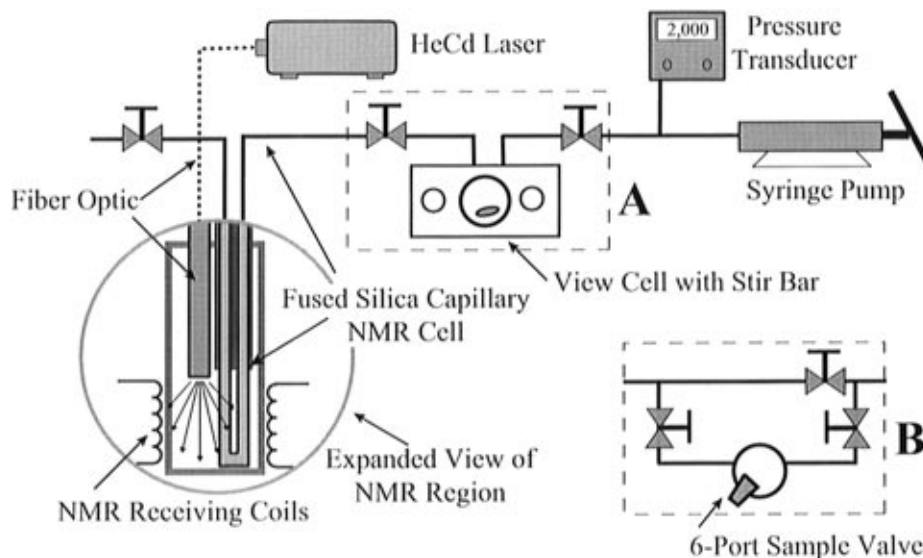


**Figure 1.** Schematic diagram of the apparatus used for *in situ* high-pressure NMR photolysis. Schematic A gives the configuration with the view cell. Schematic B shows the configuration used with a standard HPLC injection valve. After the solute is "injected" into the capillary by either method B or A the capillary HPNMR vessel can be isolated, by means of high pressure valves, from the sampling cell (view cell or HPLC valve) and pressurized to 4 kbar. The system is limited to less than 700 bars with the sampling cells in line.

high-pressure NMR in determining the fundamental dynamic and electronic properties in SCF through the investigation of the spin–lattice relaxation times,  $T_1$ , and NMR magnetic shielding constants,  $\sigma$ , of solutions of the organometallic and substituted organometallic compounds in both pure and binary mixtures of sub- and supercritical  $\text{CO}_2$  and ethylene as a function of temperature and pressure.

### Experimental Section

Cymantrene and methylcymantrene were purchased from Strem Chemical Inc. with the crystalline cymantrene being used as received and the liquid methylcymantrene distilled under reduced pressure immediately prior to use and stored under nitrogen in a freezer. The Polymer Grade ethylene (99.8%) and SFC Grade  $\text{CO}_2$  (>99.99%) were purchased from Scott Specialty Gases while the  $\text{H}_2$  was purchased from Matheson. Mixtures of gases (hydrogen in  $\text{CO}_2$ , hydrogen in ethylene, and ethylene in  $\text{CO}_2$ ) were made in the laboratory based on the weight percent of each gas.

The  $^1\text{H}$  HPNMR spectra were run at 300 MHz on a Varian VXR-300 spectrometer operating at 7.01 T with use of a standard 5 mm multinuclear, broad band probe. The  $^1\text{H}$  chemical shifts were referenced to external samples of tetramethylsilane (or  $\text{CHCl}_3$ ) at 25 °C in  $\text{CDCl}_3$ . We also used the chemical shift density dependence of ethylene as an internal chemical shift reference.<sup>9</sup> The high-pressure NMR vessel was constructed of fused silica capillary tubing (Polymicro Technologies Inc.), with either 100  $\mu\text{m}$  i.d./360  $\mu\text{m}$  o.d. for high pressures (>2000 bar) or 180  $\mu\text{m}$  i.d./360  $\mu\text{m}$  o.d. for lower pressures (<2000 bar). The HPNMR capillary was centered in a standard 5 mm NMR tube by the use of Teflon spacers. The capillary polyimide coating was carefully removed from the portion of the capillary located in the NMR detection coil region to allow for *in situ* photolysis. The photolysis was performed through the use of a fiber optic attached to a continuous wave 40 mW, 325 nm HeCd laser (LiCONiX 300 series). Measured power at the end of the fiber optic was <1 mW. The fiber optic was positioned approximately 2 cm above the section of the capillary HPNMR cell in the NMR detection coil. There were no observed interferences in the  $^1\text{H}$  NMR signal due to the fiber optic. To verify that there were no wavelength dependent anomalies, selected samples were also photolyzed outside the NMR magnet with a high-pressure mercury lamp. No detectable difference was found in the products resulting from photolysis with the broad band mercury lamp or HeCd laser.

Temperature was determined by using the thermocouple in the NMR probe. The temperature was ascertained to be accurate to  $\pm 1.0$  °C

and reproducible to  $\pm 0.1$  °C with use of standard NMR calibration methods.<sup>13</sup> Pressures were measured by using a calibrated pressure transducer (Precise Sensors, Inc) with a precision of  $\pm 0.7$  bar. All fluid densities were interpolated from literature values by using standard techniques.<sup>14,15</sup> Densities of the fluid solutions are assumed to be that of the pure fluids. No attempt was made to measure the actual densities of the fluid solutions containing the organometallic compounds. The  $T_1$  relaxation measurements were determined by the standard inversion recovery method,  $180^\circ\text{-}\tau\text{-}90^\circ$ .<sup>16</sup> Cymantrene and methylcymantrene were freeze–pump–thawed in the capillary tube prior to  $T_1$  measurements.

Three configurations of the HPNMR system were used in this study. In the first, a stainless steel mixing vessel (8 mL volume) equipped with a magnetic stir bar and sapphire windows (allowing visual inspection of the mixing) was plumbed with a high-pressure stainless steel inlet valve and a high-pressure stainless steel outlet valve hooked directly to the capillary, Figure 1A. The capillary was bent in a U shape and a pressure letdown device (High Pressure Equipment 1/16 in. valve) was plumbed onto the end of the capillary outside of the magnet and connected to a restrictor to avoid pressure gradients in the capillary cell during sample transfer. The metal complex was added to the mixing vessel under an inert atmosphere, and the system was purged with the solvent gas of choice and pressurized. The mixture was transferred into the NMR detection region for photolysis and NMR observation. Multiple pressure and temperature experiments could be performed in a very efficient manner with the products being flushed out of the detection region of the capillary by opening the restrictor valve. In the second method, liquid methylcymantrene was injected directly into the HPNMR capillary through the use of a Rheodyne HPLC valve (model 7010 sample valve), Figure 1B. The degassed liquid methyl cymantrene was syringed into a 20  $\mu\text{L}$  injection loop on the valve and then loaded into the capillary with use of normal HPLC injection procedures. A third method entailed loading solid cymantrene directly into the capillary by carefully packing the solid (<2 mg) into the end (pushed up 2 cm from the end) of a single pass capillary. The capillary was then sealed while the solid was immersed in liquid nitrogen to prevent decomposition.

(13) Van Geet, A. L. *Anal. Chem.* **1968**, *40*, 2227.

(14) Din, F. *Thermodynamic Functions of Gases, Vol. 1, Ammonia, Carbon Dioxide and Carbon Monoxide.*; Butterworths: London, 1956; pp 132–134.

(15) Angus, S.; Armstrong, B.; de Reuck, K. M. *International Thermodynamic Tables of the Fluid State Ethylene, 1972.*; Butterworths: London, 1974.

(16) Levy, G. C.; Peat, F. R. *J. Magn. Reson.* **1975**, *18*, 500.

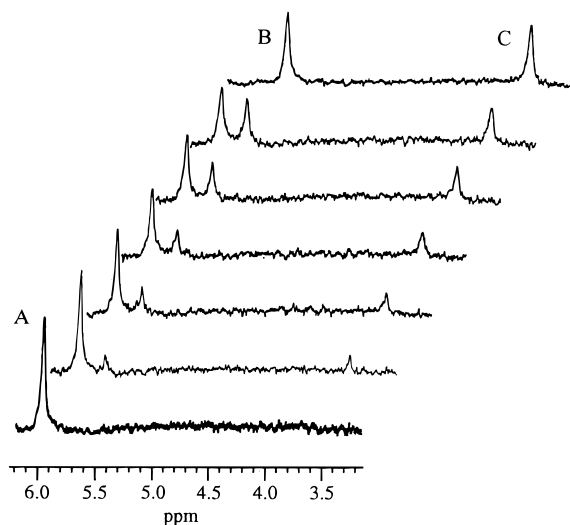


**Figure 2.** *In situ* photolysis (325 nm) of cymantrene in SCF ethylene at 25 °C and 316 bar followed by proton NMR. Total photolysis time was 10 h. Peak A (6.01 ppm) is the cyclopentadienyl protons from the reactant cymantrene, peak B (5.79 ppm) is the cyclopentadienyl protons from  $\text{CpMn}(\text{CO})_2(\eta^2\text{-C}_2\text{H}_4)$ , and peak C (3.63 ppm) is the ethylene bound to the manganese in  $\text{CpMn}(\text{CO})_2(\eta^2\text{-C}_2\text{H}_4)$ . The spectra are offset for clarity. The ethylene solvent peak is outside the displayed region at 6.68 ppm. These spectra were collected with a 45° pulse, 10 s recycle time, and a total of 32 transients with a line broadening of 2 Hz.

**Safety Note.** The high pressures and temperatures used in this study can be dangerous. Appropriate safety precautions must be observed during any high-pressure operation.

## Results and Discussion

***In Situ* Photolysis.** The time evolution of the photochemical ethylene substitution for CO on cymantrene in SCF ethylene at 25 °C and 316 bar is shown in Figure 2. The bottom spectrum in Figure 2 shows the typical  $^1\text{H}$  NMR signal obtained for the cyclopentadienyl protons (peak A, 6.01 ppm) from pure cymantrene dissolved in ethylene obtained with our standard HPNMR parameters (45° pulse, 32 transients, and a 10 s recycle time). Even at the low light flux used in this experiment the reaction is complete in the capillary within 10 h. The  $^1\text{H}$  HPNMR spectra show that the cymantrene converts to  $\text{CpMn}(\text{CO})_2(\eta^2\text{-C}_2\text{H}_4)$  with no intermediates or other products observed. The cyclopentadienyl protons (B in Figure 2, 5.79 ppm) from  $\text{CpMn}(\text{CO})_2(\eta^2\text{-C}_2\text{H}_4)$  are shifted upfield from the reactant protons. The single  $^1\text{H}$  NMR signal from the manganese bound ethylene protons (C in Figure 2) is shifted far upfield (3.63 ppm) from that of the ethylene solvent (6.68 ppm). We have confirmed the assignment of the  $\text{CpMn}(\text{CO})_2(\eta^2\text{-C}_2\text{H}_4)$  by SCF IR through comparison to previous work.<sup>4,17,18</sup> The  $^1\text{H}$  NMR of the photolysis of cymantrene in SCF ethylene at higher temperatures, 100 °C shown in Figure 3 and at 150 °C, yields the same monoethylene-substituted species,  $\text{CpMn}(\text{CO})_2(\eta^2\text{-C}_2\text{H}_4)$ . Notice the lower signal-to-noise ratio in Figure 3 at 100 °C and 317 bar than in Figure 2, at 25 °C. This is attributable to the lower overall density (0.0118 mol/cm<sup>3</sup>) and therefore smaller amount of manganese complex in the NMR detection zone at the higher temperature than at the lower temperature (0.0153 mol/cm<sup>3</sup>). These reactions were run under conditions of a constant 0.013 mol fraction of cymantrene in ethylene. The spectra obtained at 150 °C (corresponding to a density of 0.00982 mol/cm<sup>3</sup>) show lower signal-to-noise, but

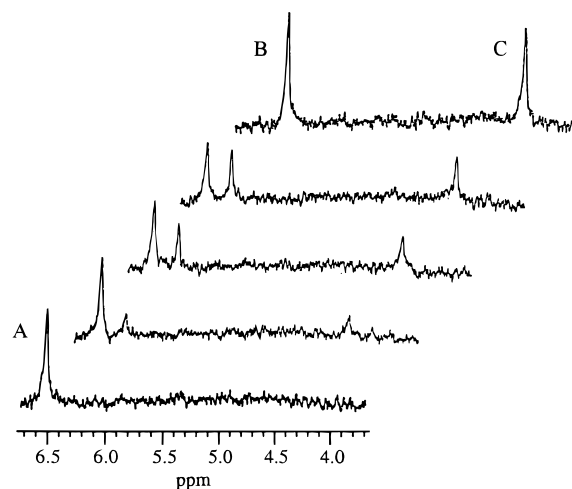


**Figure 3.** *In situ* photolysis (325 nm) of cymantrene in SCF ethylene at 100 °C and 317 bar followed by proton NMR. Peak A (6.56 ppm) is the cyclopentadienyl protons from the reactant cymantrene, peak B (6.33 ppm) is the cyclopentadienyl protons from  $\text{CpMn}(\text{CO})_2(\eta^2\text{-C}_2\text{H}_4)$ , and peak C (4.31 ppm) is the ethylene bound to the manganese in  $\text{CpMn}(\text{CO})_2(\eta^2\text{-C}_2\text{H}_4)$ . The spectra are offset for clarity. The ethylene solvent peak is outside the displayed region at 7.27 ppm. These spectra were collected with a 45° pulse, 10 s recycle time, and a total of 128 transients with a line broadening of 2 Hz.

the peaks due to the reactant cymantrene and the ethylene-substituted product could be identified with no other peaks being observable. Similar results were obtained for methylcymantrene.

Photolysis under high pressures (2609 bar corresponding to a fluid density of 0.214 mol/cm<sup>3</sup>) at 30 °C also resulted in only the monoethylene-substituted product. The same ethylene-substituted product was obtained when mixtures of ethylene in CO<sub>2</sub> were used as solvent systems. Transformations from cymantrene or methylcymantrene to their respective monoethylene-substituted complexes were observed even at very low (2:1) ethylene–cymantrene molar ratios. There were no observable temperature or pressure effects on this photolysis reaction.

Both the starting cymantrene and the ethylene-substituted complex show excellent stability in SCF ethylene over the pressure and temperature ranges investigated. These systems are stable in supercritical fluids, allowing one to examine solution dynamics and intermolecular interactions at high temperatures and high pressures. There is no evidence for decomposition or thermal substitution of ethylene, even at 150 °C or at 2700 bar in neat ethylene for cymantrene, methylcymantrene, or their ethylene-substituted products. This high thermal stability is consistent with the relatively high Mn–CO bond strength, ~47 kcal/mol, measured for cymantrene.<sup>19</sup>

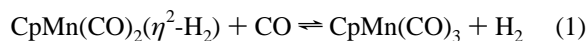
**Photolysis with H<sub>2</sub>.** Single-phase solutions containing hydrogen and methylcymantrene in SCF CO<sub>2</sub> were prepared at low hydrogen concentrations. Upon *in situ* photolysis at 325 nm or broad band *ex situ* photolysis of the reaction mixture only small amounts (<1%) of the dihydrogen complex,  $\text{CpMn}(\text{CO})_2(\eta^2\text{-H}_2)$ , reported in the literature were observed by  $^1\text{H}$  HPNMR.<sup>4</sup> The conversion of cymantrene to the dihydrogen complex is much lower than the conversion to the ethylene complex under similar conditions. While ethylene substitution for CO is rapid and proceeds to completion, only a small fraction of the cymantrene complex is converted to the dihydrogen complex,  $\text{CpMn}(\text{CO})_2(\eta^2\text{-H}_2)$ , at 25 or 35 °C.

(17) Angelici, R. J.; Loewen, W. *Inorg. Chem.* **1967**, *6*, 682–686.

(18) Hamley, P. A.; Kazarian, S. G.; Poliakov, M. *Organometallics* **1994**, *13*, 1767–1774.

(19) Klassen, J. K.; Selke, M.; Sorensen, A. A.; Yang, G. K. *J. Am. Chem. Soc.* **1990**, *112*, 1267–1268.

This apparent low conversion of  $\text{CpMn}(\text{CO})_3$  to  $\text{CpMn}(\text{CO})_2(\eta^2\text{-H}_2)$  in  $\text{SCF H}_2/\text{CO}_2$  is in contrast to those obtained by Poliakoff et al. in which almost complete conversion of the cymantrene to  $\text{CpMn}(\text{CO})_2(\eta^2\text{-H}_2)$  in  $\text{SCF H}_2/\text{CO}_2$  by photolysis was observed by IR spectroscopy.<sup>4</sup> An isolated yield of  $\text{CpMn}(\text{CO})_2(\eta^2\text{-H}_2)$  of approximately 20% was reported. One explanation for the discrepancy between our results and those previously reported could be that only a steady state equilibrium, eq 1, can be established in our nonflowing photolysis experiment.



The isolated yields previously reported were produced under nonequilibrium rapid expansion of supercritical solutions (RESS)<sup>20</sup> conditions, in which the CO produced is continuously removed from the reaction mixture as the  $\text{CpMn}(\text{CO})_2(\eta^2\text{-H}_2)$  product is cooled and precipitated.

While the dihydrogen complex may be much less soluble in the SCF solvents than the starting materials, we do not believe this to be the reason for the small amount of photolyzed product observed during these reactions. The very similar absolute intensities of the  $^1\text{H}$  NMR peak areas from the cyclopentadienyl protons on cymantrene and the lack of any line width changes before and after exhaustive photolysis demonstrate that there is little loss of the starting material due to insolubility of a product at high fluid densities.

Photolysis of mixtures of hydrogen and methylcymantrene dissolved in SCF ethylene always led to the ethylene-substituted complex. There was no evidence for the dihydrogen manganese complex or for ethane production.

**Phase Behavior of Binary Systems.** The HPNMR system allows direct insight into solubility limits and phase behavior, including the mole fractions of components in each phase, by direct comparison of the  $^1\text{H}$  NMR peak areas of each component. To determine the saturation limit of methylcymantrene in ethylene 1.5 mL of methylcymantrene was loaded into the 8 mL stainless steel view cell which was sealed and pressurized to 275 bar with ethylene. The mixture was observed visually through the sapphire windows to be two phase even after 24 h of stirring. The upper, lightly colored, ethylene-rich, methylcymantrene saturated phase was sampled by means of a capillary HPNMR dip tube. At 25 °C the mole fraction of  $\text{MeCpMn}(\text{CO})_3$  in the methylcymantrene-in-ethylene saturated solution was measured by proton NMR to be 0.061 at 275 bar. This corresponds to a saturated methylcymantrene concentration of 0.95 M at an ethylene fluid density of 0.0152 mol/cm<sup>3</sup>.

*In situ* photolysis at 25 °C of this saturated solution led to phase separation in the capillary HPNMR cell after greater than 90% conversion of the methyl cymantrene. New broad peaks were observed to grow in the  $^1\text{H}$  NMR spectrum separate from those expected for the methyl-cymantrene reactant or the  $\text{MeCpMn}(\text{CO})_2(\eta^2\text{-C}_2\text{H}_4)$  product. The broad peaks were resolved by cooling the sample to 0 °C, and the spectrum shown in Figure 4A was obtained. This spectrum shows two-phase behavior for this system with almost a 1 ppm difference in the chemical shifts between similar protons in the two phases. This large chemical shift disparity suggests a rather large difference in the fluid density of the two phases (see discussion on chemical shifts below). This mixture has separated into an ethylene-rich phase, peaks a–d, and a  $\text{MeCpMn}(\text{CO})_2(\eta^2\text{-C}_2\text{H}_4)$ -rich phase, peaks w–z. The ethylene-rich phase is very similar to the initial single phase ethylene solvent system, as can be seen when

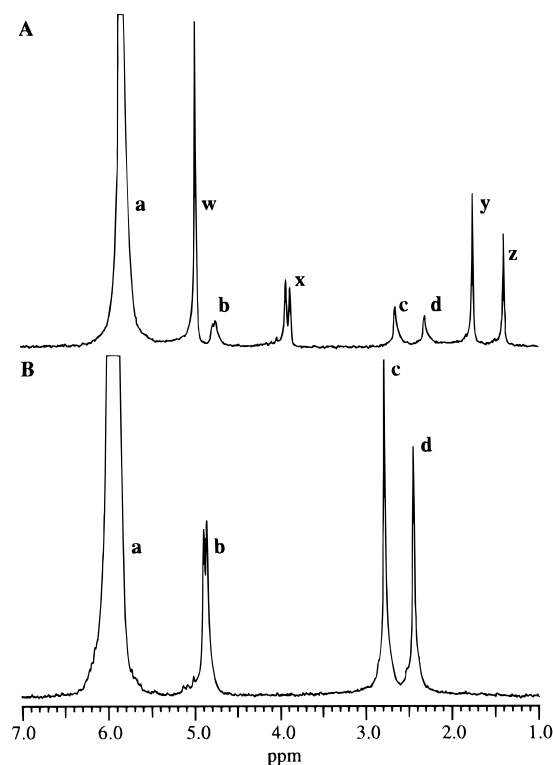


**Figure 4.** (A) Proton NMR spectrum of a two-phase system of  $\text{MeCpMn}(\text{CO})_2(\eta^2\text{-C}_2\text{H}_4)$  and ethylene at 0 °C under 274 bar of pressure. Peaks a (ethylene), b ( $\alpha\text{-Cp}$  and  $\beta\text{-Cp}$ ), c (methyl), and d (ethylene bound to manganese) are from the ethylene-rich phase. Peaks w (ethylene), x ( $\alpha\text{-Cp}$  and  $\beta\text{-Cp}$ ), y (methyl), and z (ethylene bound to manganese) are from the  $\text{MeCpMn}(\text{CO})_2(\eta^2\text{-C}_2\text{H}_4)$ -rich phase. (B) At elevated temperatures (>25 °C) the system became one-phase. The small peaks to the left of the cyclopentadienyl protons are from unreacted methylcymantrene. These spectra were obtained with a 45° pulse, 10 s recycle delay, and 32 transients with a line broadening of 2 Hz.

compared to Figure 4B obtained at 35 °C. The slight change in chemical shifts between the 35 °C spectrum and the 0 °C spectrum for the a–d peaks is due to the temperature and density changes between the two samples. These spectra were collected at a constant pressure of 274 bar.

This  $^1\text{H}$  HPNMR technique allows the *in situ* quantification of the multi-phase systems. The ethylene-rich phase was found to comprise 83% of the observable protons (from both ethylene and  $\text{MeCpMn}(\text{CO})_2(\eta^2\text{-C}_2\text{H}_4)$ ). The mole ratio,  $\text{MeCpMn}(\text{CO})_2(\eta^2\text{-C}_2\text{H}_4)$ -to-ethylene, was much lower, 0.036, than in the  $\text{MeCpMn}(\text{CO})_2(\eta^2\text{-C}_2\text{H}_4)$ -rich phase in which the ratio was 0.45. It is of interest to note that the second phase was not pure  $\text{MeCpMn}(\text{CO})_2(\eta^2\text{-C}_2\text{H}_4)$  but an almost 1:1 mixture of  $\text{MeCpMn}(\text{CO})_2(\eta^2\text{-C}_2\text{H}_4)$  and ethylene. This phase composition is consistent with the large differences in chemical shift observed. The manganese-rich phase is more dense than the ethylene-rich phase based on the observed chemical shifts.

This result leads to the surprising conclusion that  $\text{MeCpMn}(\text{CO})_2(\eta^2\text{-C}_2\text{H}_4)$  is less soluble in ethylene than methyl cymantrene, possibly due to enhanced polarity of the complex through changes in its dipole moment as the carbonyl ligand is replaced. A second possible explanation of the phase separation is that the removal of ethylene and release of carbon monoxide into the solvent system reduces the solubilizing power of the solvent. Carbon monoxide is a much poorer solvent than ethylene, and its release into the solvent could cause this phase change, and since the solution is already at the saturation point, a very small perturbation of the solvent make-up could cause significant changes in the phase behavior. This result shows that caution

(20) Matson, D. W.; Fulton, J. L.; Petersen, R. C.; Smith, R. D. *Ind. Eng. Chem. Res.* **1987**, *26*, 2298–2306. Matson, D. W.; Petersen, R. C.; Smith, R. D. *J. Mater. Sci.* **1987**, *22*, 1919–1928.

must be taken to monitor the phase behavior over the course of the reaction in SCF since assumptions that a reaction mixture will remain one phase throughout the reaction are not always valid. Small changes in composition and temperature caused a major change in the phase behavior in this study. The change in pressure as a SCF solvent or reactant is consumed or produced could also lead to phase changes. The phase behavior described here was a very localized phenomena over a very small region of the capillary HPNMR cell that was in the RF coil. The two-phase system was removed, as observed by one-phase NMR signals at all temperatures, by flowing the affected region out the NMR detection region.

**Phase Behavior of Ternary Systems.** Phase behavior of ternary systems, such as hydrogen and methylcymantrene in ethylene, or hydrogen and methylcymantrene in CO<sub>2</sub>, could also be described visually in the view cell, at low pressures, or by <sup>1</sup>H HPNMR at high pressures. A dilute homogeneous solution of methylcymantrene in ethylene, total pressure 138 bar, was prepared in the view cell and observed to be single phase by visual inspection and <sup>1</sup>H HPNMR. Upon addition of 35 bar of hydrogen the system became three phase and did not change after extensive mixing. (Similar phase effects due to hydrogen addition have been previously noted.<sup>7</sup>) By visual inspection the three phases were the following: an upper phase with very little color; a middle phase with more color; and a highly colored lower phase. By <sup>1</sup>H HPNMR we were able to determine that the upper phase was composed of mainly hydrogen in ethylene. Even though the phase was slightly colored by the methylcymantrene we were unable to detect any peaks attributable to the metal complex. The middle phase was composed of methylcymantrene-in-ethylene with little if any hydrogen, and the bottom phase was a methylcymantrene-rich phase containing ethylene as discussed above. In this particular system the hydrogen greatly reduced the solvating power of the SCF ethylene. At higher ethylene pressures (concentrations) and lower methylcymantrene concentrations we were able to observe single-phase behavior for this ternary system. But, we generally found it difficult to prepare solutions in which all three components, hydrogen, methylcymantrene, and ethylene, were present in the HPNMR cell in detectable amounts. Similar phase behaviors for cymantrene or methylcymantrene and hydrogen were obtained with CO<sub>2</sub>-based systems. There was no analogous decrease in solvating power with mixtures of ethylene and CO<sub>2</sub>. These phase behavior experiments show the utility of high-pressure NMR for obtaining quantitative data concerning solubilities and phase dynamics in these systems.

**Chemical Shifts and Relaxation Times.** The <sup>1</sup>H HPNMR spectra of methylcymantrene dissolved in supercritical ethylene, a binary mixture of ethylene in CO<sub>2</sub> and in CDCl<sub>3</sub>, are shown in Figure 5. Ethylene was present as a reactive solute and internal chemical shift reference in CO<sub>2</sub> during the photolysis and spin relaxation experiments. Notice that while the general features of the spectra and relative peak positions remain the same, the actual chemical shifts of the solute species in the different solvents show dramatic differences. The large disparities of chemical shifts shown in Figure 5 are primarily due to differences in solute-solvent interactions and to solvent fluid densities (CO<sub>2</sub> is more dense than ethylene under similar conditions of pressure and temperature). The chemical shifts,  $\delta_{\text{obs}}$ , of all the protons observed show a linear dependence on density over the pressure range studied, 276 to 2609 bar as shown for methyl cymantrene and ethylene at 35 °C in Figure 6. In Figure 6, parts A, B, and C, the filled symbols are the

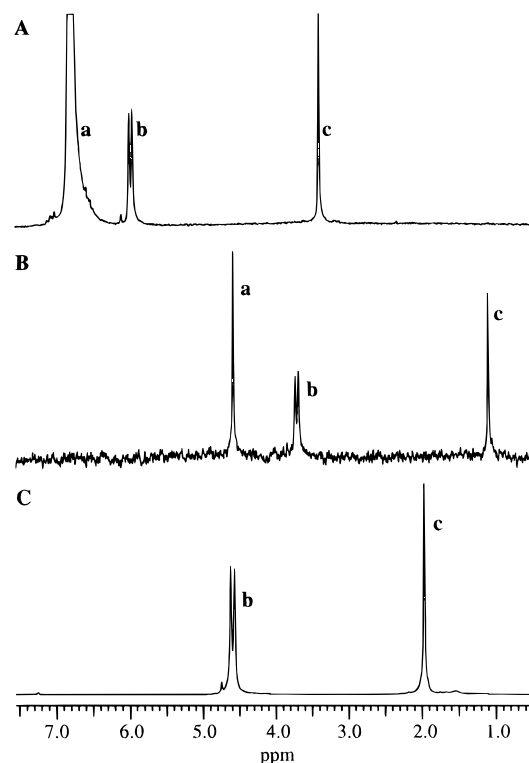


**Figure 5.** The <sup>1</sup>H NMR spectra, collected at 300 MHz, of methylcymantrene dissolved in SCF ethylene at 163 bar (upper), subcritical CO<sub>2</sub> at 276 bar (middle), and CDCl<sub>3</sub> at atmospheric pressure (lower). All the spectra were obtained at 25.0 °C. A small amount of ethylene was present in the CO<sub>2</sub>. The peaks labeled b are the protons  $\alpha$  and  $\beta$  to the methyl group on the cyclopentadienyl ring and c is the methyl group. Peaks labeled a are from ethylene.

observed chemical shifts for the protons on ethylene, the cyclopentadienyl ring, and the methyl substituent, respectively, in pure ethylene at 35 °C. The open symbols in these plots represent the chemical shifts for the same solute protons in supercritical CO<sub>2</sub>. The difference in the slopes between ethylene and CO<sub>2</sub> is due to the different intermolecular interactions of the respective solvent with the solute, see discussion below. Table 1 shows the slopes and intercepts for linear least-squares regression of the chemical shifts as a function of density for three different temperatures. Notice that the intercepts (or  $\sigma_0(T)$ ) at zero solvent density are independent of solvent type and solely dependent on the rotational, vibrational states of the solute molecule at the temperature investigated. The intercept,  $\sigma_0(T)$ , for ethylene in both pure ethylene and the binary mixture in CO<sub>2</sub> is comparable to that reported earlier by Trappeniers and Oldenziel.<sup>22</sup> The isotherms of the methyl group on methylcymantrene for temperatures between -40 and 100 °C are shown in Figure 7. Similar linear isotherms for all the protons on cymantrene, methyl cymantrene, and ethylene in CO<sub>2</sub> can be plotted over the entire temperature and pressure range studied.

Chemical shifts give a detailed understanding of solvation effects on the solute. On a molecular level the magnetic shielding constant,  $\sigma$ , is an absolute measure of the electronic contribution to the observed nuclear magnetic moments which are sensitive to the chemical environment.<sup>21</sup> As pointed out by Jameson, in a comprehensive review of gas-phase NMR spectroscopy, the shielding is a second order molecular property as are magnetizability and polarizability. Generally,  $\sigma$ , for a compressed gas, such as ethylene, is written in terms of density,  $\rho$ , using a virial expansion of the form:

(21) Jameson, C. J. *Chem. Rev.* **1991**, *91*, 1375.

(22) Trappeniers, N. J.; Oldenziel, J. G. *Physica* **1976**, *82A*, 581-595.

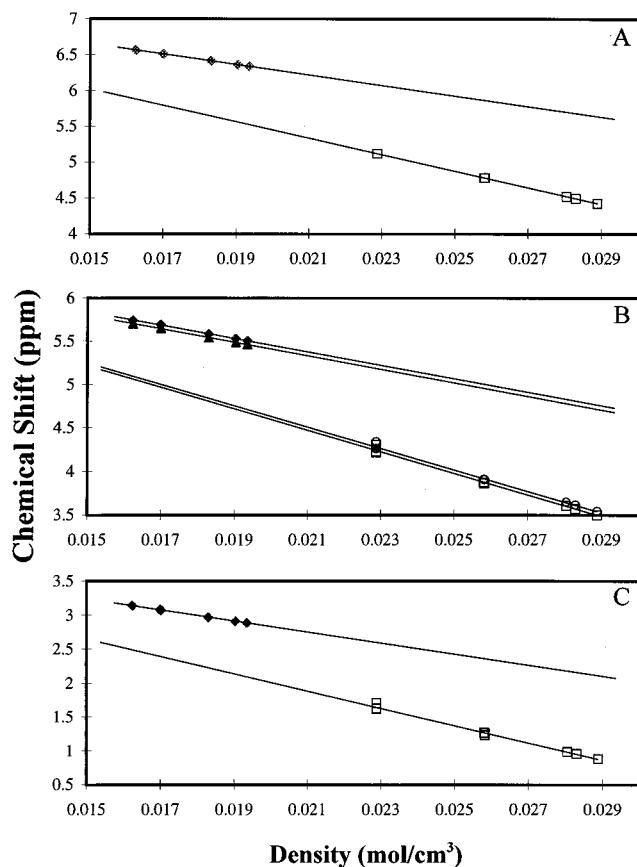


**Figure 6.** Proton NMR chemical shift isotherms for methylcymantrene dissolved in ethylene (filled symbols) and in CO<sub>2</sub> (open symbols) at 35 °C. The chemical shifts of methyl (trace C),  $\alpha$ -Cp and  $\beta$ -Cp protons (trace B) and ethylene (trace A) all show a linear chemical shift dependence on density over the pressure range, 170–2609 bar, studied.

**Table 1.** Chemical Shifts of Ethylene and Methylcymantrene Described as a Linear Function of Solvent Density in CO<sub>2</sub> and Ethylene at -40, 35, and 60 °C<sup>a</sup>

proton	ethylene			CO <sub>2</sub>		
	$\sigma^b$	$\sigma_{loc1}^c$	$\sigma_0^d$	$\sigma^b$	$\sigma_{loc1}^e$	$\sigma_0^d$
60 °C						
ethylene	74 ± 1	-8.5	7.7 ± 0.1	115 ± 1	27.9	7.7 ± 0.1
$\alpha$ -Cp	76 ± 2	-6.5	6.89 ± 0.03	118 ± 1	30.9	6.89 ± 0.01
$\beta$ -Cp	77 ± 2	-5.5	6.88 ± 0.03	119 ± 1	31.9	6.89 ± 0.01
methyl	78 ± 2	-4.5	4.32 ± 0.03	122 ± 1	34.9	4.36 ± 0.02
35 °C						
ethylene	74 ± 1	-8.5	7.77 ± 0.04	116 ± 1	28.9	7.8 ± 0.1
$\alpha$ -Cp	79 ± 2	-3.5	6.98 ± 0.04	124 ± 2	36.9	7.07 ± 0.01
$\beta$ -Cp	77 ± 2	-5.5	7.00 ± 0.04	123 ± 2	35.9	7.09 ± 0.01
methyl	81 ± 1	-1.5	4.45 ± 0.04	128 ± 1	40.9	4.56 ± 0.02
-40 °C						
ethylene	74.8 ± 0.1	-7.7	8.0 ± 0.1	121 ± 3	33.9	8.2 ± 0.1
Cp $\alpha$	77 ± 4	-5.5	7.2 ± 0.1	122 ± 3	34.9	7.3 ± 0.1
Cp $\beta$	77 ± 6	-5.5	7.1 ± 0.1	123 ± 3	35.9	7.3 ± 0.1
methyl	76 ± 5	-6.5	4.6 ± 0.1	126 ± 4	38.9	4.8 ± 0.1

<sup>a</sup> Uncertainties are reported as one standard deviation. <sup>b</sup> Measured in this study, units of ppm cm<sup>3</sup>/mol. <sup>c</sup> Calculated with  $\sigma_b = 82.5$  ppm cm<sup>3</sup>/mol; units of ppm cm<sup>3</sup>/mol. <sup>d</sup> Extrapolated to zero density relative to TMS; units of ppm. <sup>e</sup> Calculated with  $\sigma_b = 87.1$  ppm cm<sup>3</sup>/mol; units of ppm cm<sup>3</sup>/mol.

$$\sigma(T, \rho) = \sigma_0(T) + \sigma_1(T)\rho + \sigma_2(T)\rho^2 + \dots \quad (2)$$

where  $\sigma_0$  is a measure of the contribution from rotational and vibrational intramolecular dynamics of the isolated gas molecule,  $\sigma_1$  is an approximate measure of the effects of pairwise interactions, and  $\sigma_2$  represents the effect of multibody interac-

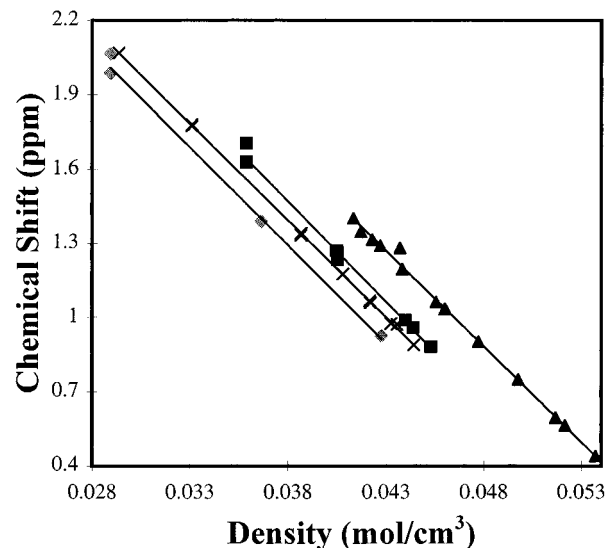


**Figure 7.** Proton NMR chemical shift (ppm) isotherms for the methyl protons on methyl cymantrene dissolved in CO<sub>2</sub> over the pressure range from 170 to 2609 bar plotted as a function of molar solvent density. Each parallel line represents one temperature, -40 (▲), 35 (■), 60 (×), and 100 °C (◆).

tions. Previous studies of the density dependence of the proton chemical shift in ethylene have shown that for lower densities (<2.5 kbar), the linear term is sufficient to describe the shielding as a function of density.<sup>22</sup> At higher densities deviation of the linear dependence of  $\sigma$  on density was observed and the second-order terms of eq 1 were necessary. Our assumption that the linear term in the virial expansion is sufficient to describe the intermolecular interactions of the solutes in the present study is justified by the strictly linear density dependence of chemical shift shown in Figure 6. Since  $\delta_{obs}$  and  $\sigma$  differ by an additive constant,  $\sigma_0$ , the chemical shift relative to an isolated molecule can be written in terms of the individual contributions as<sup>23</sup>

$$\delta_{obs} = \sigma - \sigma_0 = (\sigma_{b1} + \sigma_{loc1})\rho - \sigma_0 = (\sigma_{b1} + \sigma_{W1} + \sigma_{ex1} + \sigma_{E1} + \sigma_{a1})\rho - \sigma_0 \quad (3)$$

where  $\sigma_{b1}$  is the bulk magnetic susceptibility contribution. The local shielding contribution,  $\sigma_{loc1}$ , is a combination of  $\sigma_{W1}$ , which is due to the van der Waals dispersion interaction,  $\sigma_{ex1}$ , the contribution due to short-range exchange interactions,  $\sigma_{E1}$ , the contribution to permanent electronic interactions, and  $\sigma_{a1}$ , the contribution from magnetic anisotropy. Accordant with previous studies we assume that  $\sigma_{E1}$  and  $\sigma_{a1}$  make negligible contributions for the ethylene and CO<sub>2</sub> solvents.<sup>22,24</sup> The term  $\sigma_{ex1}$  is also assumed to be negligible as according to *ab initio* calculations by Jameson and de Dios this term is not sampled at the intermolecular distances attained in the present work.<sup>25</sup> The bulk susceptibility term,  $\sigma_{b1}$ , can be calculated according to Smith and Raynes, eq 4.<sup>26,27</sup>

$$\sigma_{b1} = -\left(\frac{4}{3}\right)\pi\chi_m \quad (4)$$

The term  $\chi_m$  is the molar magnetic susceptibility, experimentally

(23) Pfund, D. M.; Zemanian, T. S.; Linehan, J. C.; Fulton, J. L.; Yonker, C. R. *J. Phys. Chem.* **1994**, *98*, 11846–11857.

(24) Lim, Y.-H.; Nugara, N. E.; King, A. D. *J. Phys. Chem.* **1993**, *97*, 8816.

(25) Jameson, C. J.; de Dios, A. C. *J. Chem. Phys.* **1992**, *97*, 417.

(26) Bennet, B.; Raynes, W. T. *Magn. Reson. Chem.* **1991**, *29*, 946–954.

(27) Smith, A.; Raynes, W. T. *J. Crystallogr. Spectrosc. Res.* **1983**, *13*, 77.

measured to be  $-19.7 \times 10^{-6} \text{ cm}^3/\text{mol}$  for ethylene and  $-20.8 \times 10^{-6} \text{ cm}^3/\text{mol}$  for  $\text{CO}_2$ .<sup>28</sup> This leads to values of  $\sigma_{\text{b1}} = 82.5$  and  $87.1 \text{ ppm cm}^3/\text{mol}$  for ethylene and  $\text{CO}_2$ , respectively.<sup>26</sup> By subtracting these values from  $\sigma_1$  we arrive at  $\sigma_{\text{loc1}}$ , which in the present case is assumed to be a result of the pairwise dispersion interactions the nucleus is experiencing. The values of  $\sigma_{\text{loc1}}$  in ethylene and in  $\text{CO}_2$  are given in the third and sixth columns of Table 1. The values of  $\sigma_{\text{loc1}}$  for ethylene in ethylene are comparable to those previously obtained by others.<sup>27</sup> We report a more deshielded  $\sigma_{\text{loc1}}$  for ethylene than for  $\text{CO}_2$ . This implies that ethylene as a solvent has more of an "attractive" contribution to the van der Waals dispersion term relative to  $\text{CO}_2$  for the protons examined.<sup>29</sup>

The chemical shift constants  $\sigma_1$  and  $\sigma_{\text{loc1}}$  always increase in the following order: ethylene < Cp protons < methyl protons in either  $\text{CO}_2$  or ethylene solvents, Table 1. Since  $\sigma_1$  and  $\sigma_{\text{loc1}}$  are a description of the local solvent/solute interactions, then one might infer that more "attractive" (i.e. more negative/more deshielded)  $\sigma_{\text{loc1}}$  values imply greater solvent/solute interactions. This observation may allow the "tuning" of solute functionalities to optimize solute solubility in SCF, in particular in SCF  $\text{CO}_2$ , by chemical substitution at the moieties which have the least attractive solute/solvent interactions based on the experimentally determined  $\sigma_{\text{loc1}}$  values (e.g., in the present case the  $-\text{CH}_3$  functionality in methylcymantrene).

The  $\sigma_0$  temperature dependence is roughly  $-0.0026 \text{ ppm}/^\circ\text{C}$  for the methyl and  $-0.0020 \text{ ppm}/^\circ\text{C}$  for the  $\alpha$ -Cp protons on methylcymantrene in  $\text{CO}_2$  or ethylene solvent. The protons  $\beta$  to the methyl group show a slightly greater chemical shift dependence with temperature,  $-0.0031 \text{ ppm}/^\circ\text{C}$ . This difference in temperature dependence between the  $\alpha$ -Cp and the  $\beta$ -Cp protons eventually leads to the overlap of their  $^1\text{H}$  NMR signals above  $60^\circ\text{C}$ . The chemical shift difference between the  $\alpha$ -Cp and  $\beta$ -Cp protons on methylcymantrene changes with temperature and solvent density as was noted above, but the chemical shift difference between the  $\alpha$ -Cp and  $\beta$ -Cp protons on  $\text{MeCpMn}(\text{CO})_2(\eta^2\text{-C}_2\text{H}_4)$  does not change significantly, Figure 8. As density increased (temperature decreased) the chemical shift difference between the  $\alpha$ - and  $\beta$ -Cp protons on methylcymantrene increased while the difference on ethylene-substituted complex remained approximately the same. This behavior is most likely due to both a kinetic and a solvation effect caused by the change in the electron distribution in the organometallic complex through ethylene substitution and the variation in solvation of the ethylene-substituted complex by ethylene as compared to methylcymantrene.

**Relaxation Behavior.** Relaxation times ( $T_1$ ) were determined for the ethylene-substituted complexes in SCF ethylene as a function of solvent density as shown in Figure 9. The relaxation times for ethylene in this system were slightly shorter than earlier reported values for pure ethylene.<sup>30</sup> It has been suggested that the  $T_1$  values of our HPNMR vessel design have the potential for error because the observed molecules could diffuse out of the NMR detection zone prior to acquisition.<sup>31</sup> This does not appear to be a problem considering the excellent agreement with data from previous studies. There appears to be little difference in the  $T_1$ 's of similar protons on methylcymantrene and on  $\text{MeCpMn}(\text{CO})_2(\eta^2\text{-C}_2\text{H}_4)$ . The bound ethylene  $T_1$  varies from 3 to 7.5 s over a density range of 0.015 to 0.021  $\text{mol}/\text{cm}^3$ . The value of the relaxation time for the ethylene substituent is similar

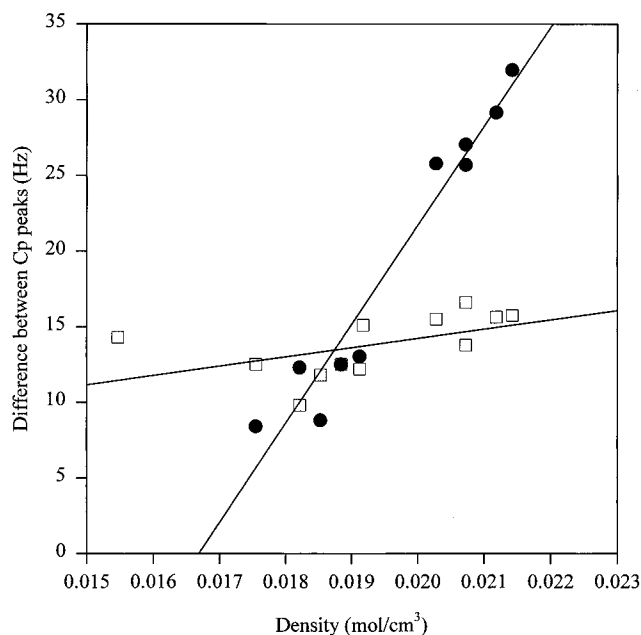


**Figure 8.** The chemical shift difference (Hz) between the  $\alpha$  and  $\beta$  cyclopentadienyl protons on methyl cymantrene (●) and  $\text{MeCpMn}(\text{CO})_2(\eta^2\text{-C}_2\text{H}_4)$  (□) dissolved in ethylene over a temperature range from  $-40$  to  $60^\circ\text{C}$ .

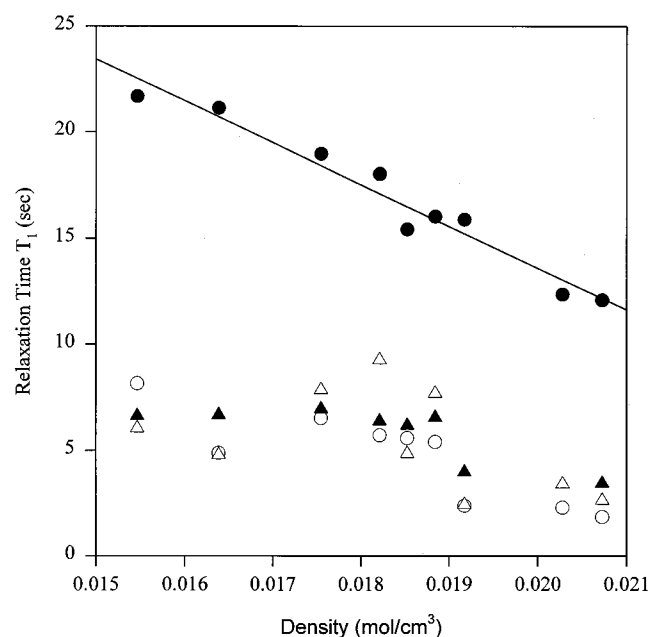


**Figure 9.** The solvent density dependence of spin-lattice relaxation times ( $T_1$ ) of methyl and ethylene protons from ethylene,  $\text{MeCpMn}(\text{CO})_3$ , and  $\text{MeCpMn}(\text{CO})_2(\eta^2\text{-C}_2\text{H}_4)$  in ethylene solvent. The unbound ethylene (●) shows linear dependence with density. The methyl protons from methyl cymantrene (▲) and  $\text{MeCpMn}(\text{CO})_2(\eta^2\text{-C}_2\text{H}_4)$  (△) and the bound ethylene on  $\text{MeCpMn}(\text{CO})_2(\eta^2\text{-C}_2\text{H}_4)$  (○) show a nonlinear density dependence.

to those of the other protons on the two complexes. This investigation is the first *in situ* determination of solution dynamics of ethylene-substituted organometallics in SCF and displays the expected decrease in  $T_1$  for ethylene substituted for the carbonyl group on the organometallic relative to the  $T_1$  value of pure, unbound ethylene. This is consistent with an enhanced intramolecular relaxation mechanism anticipated for the  $^1\text{H}$  nuclei through quadrupole relaxation processes with  $^{55}\text{Mn}$ . In general, the  $T_1$  relaxation times for methylcymantrene in both ethylene and  $\text{CO}_2$  increase with decreasing fluid density.

(28) Landolt, H. H.; Bornstein, R. *Zahlenwerte und Funktionen*; Springer-Verlag: Berlin, 1951; Vol. II, Part 3.

(29) Rummens, F. H. A.; Bernstein, H. J. *J. Chem. Phys.* **1965**, *43*, 2971.

(30) Trappeniens, N. J.; Prins, K. O. *Physica* **1967**, *33*, 435-438.

(31) Bai, S.; Taylor, C. M.; Mayne, C. L.; Pugmire, R. J.; Grant, D. M. *Rev. Sci. Instrum.* **1996**, *67*, 240-243.

This is the first study of spin–lattice relaxation of substituted ethylene on organometallic compounds in supercritical fluids and more data are needed to allow a complete analysis of longitudinal relaxation processes in these solutions.

### Conclusions

We have demonstrated the first *in situ* photolysis of organometallic species with on-line NMR detection of the reaction products and direct observation of the substituted ligand attached to the metal center. These experiments were easily performed over a wide range of temperatures and pressures by using a standard NMR probe with the HPNMR capillary pressure vessels. The photochemical reaction of manganese carbonyls with ethylene proceeded to the monoethylene-substituted complex with no other observed products even under extreme conditions. Dihydrogen substitution for CO was observed, but does not appear to proceed to high conversions in CO<sub>2</sub>. Hydrogen was found to be a poor solvent for these organometallic complexes, and small amounts in either CO<sub>2</sub> or ethylene

can precipitate the metal complex from solution or cause phase separation. The photochemical studies of H<sub>2</sub> and cymantrene described in this paper differ from earlier reported spectroscopic investigations in that a steady-state equilibrium was established between the products and reactants in the HPNMR experiments. This is believed to contribute to the different product distributions described in this effort as compared to the IR flow-through reactor design described in the literature.<sup>4</sup> The HPNMR system described also allows one to spectroscopically probe multiphase systems and determine the compositions of the phases *in situ*. This can be a valuable aid for investigations of catalytic and stoichiometric reactions of organometallic complexes in SCF.

**Acknowledgment.** Work at the Pacific Northwest National Laboratory (PNNL) was supported by the Office of Energy Research, Office of Basic Energy Sciences, Chemical Sciences Division of the U.S. Department of Energy, under contract DE-ACO676RLO 1830.

JA9711876